

# 行政院國家科學委員會專題研究計畫 期中進度報告

## 子計畫九：固態微波元件、電路模型及分析(2/3)

計畫類別：整合型計畫

計畫編號：NSC91-2219-E-009-050-

執行期間：91年08月01日至92年07月31日

執行單位：國立交通大學電信工程學系

計畫主持人：孟慶宗

計畫參與人員：孟慶宗、彭安賢

報告類型：精簡報告

處理方式：本計畫可公開查詢

中 華 民 國 92 年 5 月 30 日

行政院國家科學委員會專題研究計劃期中報告

※※※

※ 固態微波元件 電路模型及分析 (2/3) ※

※ Model and analysis of millimeter-wave device and circuit (2/3) ※

※※※

計劃類別:  個別型計劃  整合型計劃

計劃編號: NSC 91-2219-E-009-050

執行期間: 91 年 8 月 1 日 92 年 7 月 31 日

計劃主持人: 孟慶宗

本成果包含以下應繳交文件:

赴國外出差或研習心得報告一份

赴大陸地區出差或研習心得報告一份

出席國際學術會議心得報告及發表論文各一份

國際合作研究計劃國外研究報告一份

執行單位: 國立交通大學電信系

中華民國: 92 年 5 月 20 日

# 行政院國家科學委員會專題研究計劃期中報告

## 固態微波元件、電路模型及分析

### Model and analysis of millimeter-wave device and circuit

計畫編號: NSC 91-2219-E-009-050

執行期限: 91年8月1日至92年7月31日

主持人: 孟慶宗 國立交通大學電信系

計畫參與人員: 孟慶宗、彭安賢

#### 一、中文摘要

應變晶格高移動度電晶體的平均閘極電流和汲極電流可以用來預估應變晶格高移動度電晶體的不同增益壓縮機制。其中包括：膝電壓、夾止電壓、崩潰電壓、和最大電流輸出所造成的不同增益壓縮機制。在這裡，我們找到了不同的增益壓縮機制各有其獨特的平均閘極電流和汲極電流特徵。如此一來，有利於我們找出固態微波元件中的應變晶格高移動度電晶體的增益壓縮機制電路模型。

#### Abstract

Average rf gate and drain currents can be used to determine gain compression mechanisms for PHEMTs with different pinch-off voltages. Knee voltage, pinch-off voltage, breakdown voltage and  $I_{max}$  clip output I-V waveform of a PHEMT and cause gain compression. We found that there is a distinct signature in average rf gate and drain currents to characterize each gain compression mechanism in PHEMTs. A PHEMT with low pinch-off voltage behaves the same in rf gate and drain currents as a PHEMT with high pinch-off voltage in pinch-off voltage, knee voltage and breakdown voltage gain compression mechanisms, but behaves differently in  $I_{max}$  gain compression mechanisms.

#### 二、計畫緣由與目的

Knee voltage, pinch-off voltage, breakdown voltage and  $I_{max}$  clip output I-V waveform of a PHEMT and cause gain compression and power saturation. Meng et al have successfully used rf gate and drain currents near  $P_{1dB}$  to determine gain compression mechanisms in MESFET [1]. The same approach is used to characterize AlGaAs/InGaAs/GaAs PHEMTs gain compression mechanism in this paper. A PHEMT device differs from a MESFET device in the transconductance characteristics. In the case of a MESFET device, transconductance becomes higher when gate voltage is biased more positively. On the other hand, a PHEMT device has a maximum transconductance at a certain gate voltage because a parasitic low mobility AlGaAs MESFET starts to conduct and degrades transconductance when the gate voltage is biased beyond the maximum transconductance region. Thus, gain compression

mechanisms of two types of AlGaAs/InGaAs/GaAs PHEMTs with different pinch-off voltages are studied in this work.

### 三. 研究成果與方法

The two kinds of AlGaAs/InGaAs/GaAs PHEMT devices are from the same epi-wafer and were intentionally etched differently to obtain different  $I_{dss}$  while the rest of process parameters were kept identical. Gate length is 0.35  $\mu\text{m}$ . The high current PHEMT device has 2.5 V pinch-off voltage and maximum transconductance occurs at  $V_{gs}=-1.5$  V while the low current PHEMT device has 1.5 V pinch-off voltage and maximum transconductance occurs at  $V_{gs}=-0.3$ V. A low pinch-off voltage PHEMT device has higher gate-to-drain breakdown voltage and thus becomes harder to observe the breakdown gain compression mechanism. I-V curves of the PHEMT device with high pinch-off voltage (150  $\mu\text{m}$  gate width) and the PHEMT device with low pinch-off voltage (250  $\mu\text{m}$  gate width) are illustrated in figure 1 and figure 2, respectively.

### 四. 結果與討論

The input tuner impedance is set to maximize small signal gain while the output tuner impedance is set to maximize output power at a strong enough input power under load-pull condition. A commercial ATN load pull system is used here to acquire experimental data and all the measurements were performed at 1.8 GHz in this section. Large signal performances as a function of input power are then measured at each bias point. The exact loadline impedance does not affect gain compression mechanism when a device is biased very close to the gain compression region. Four bias points near only one gain compression region were selected for the PHEMT device with high pinch-off voltage. Figure 3 illustrates power performance, the average rf gate and drain current as a function of input power when  $V_{ds}=2$ V  $V_{gs}=-1.5$  V (near knee voltage). The average rf gate current is zero and average drain and average drain current becomes smaller when gain compression (near  $P_{1dB}$ ) occurs. The gate current is still zero even at higher gain compression point. In other words, gate is not forward-biased when knee voltage clips output waveform. The power performance and average rf currents when biased at  $V_{ds}=3$ V  $V_{gs}=-2.5$ V (near pinch-off voltage) are illustrated in figure 4. The operation changes from class A to class AB as input signal becomes larger. Thus, the average drain current increases near  $P_{1dB}$ . However, gate current is zero because gate is still in reverse bias when gain compression occurs. Breakdown voltage can also cause gain compression and is illustrated in figure 5 for the case of  $V_{ds}=5$ V  $V_{gs}=-2.5$ V (near breakdown voltage). Strictly speaking, figure 5 corresponds to a mixed gain compression mechanism because the device experiences pinch-off voltage gain compression slightly before the breakdown voltage gain compression mechanism. The average rf gate current becomes negative and the average rf drain current increases near  $P_{1dB}$ . The increase in drain current comes from the generation of positive drain current by avalanche at large drain voltage swing. Also, there exists negative gate current flowing into the gate when the large drain voltage swing reaches breakdown voltage. Figure 6 illustrates power performance and the average rf current when  $V_{ds}=4$ V  $V_{gs}=-1.5$ V (near  $I_{max}$ ). The average rf gate

current is zero and average drain current decreases when gain compression (near  $P_{1dB}$ ) occurs because the maximum transconductance occurs at  $V_g = -1.5$  V. A low  $V_p$  PHEMT device behaves differently in  $I_{max}$  gain compression mechanism as illustrated in figure 7. The drain current decreases and gate current starts to increase near  $P_{1dB}$  in figure 7. Figure 8 illustrate the knee voltage and pinch-off voltage gain compression mechanisms for a low  $V_p$  PHEMT device. As it can be observed in figure 4, 6, and 7, the gate current at  $P_{1dB}$  is closer to the positive gate current region in the case of a low pinch-off PHEMT device because maximum transconductance voltage occurs more toward forward gate conducting voltage.

In summary, all the gain compression mechanisms and their associate signatures for PHEMT devices have been discussed. A low  $V_p$  PHEMT device behaves the same in rf gate and drain currents as a high  $V_p$  PHEMT device in pinch-off voltage, knee voltage and breakdown voltage gain compression mechanisms, but differs in  $I_{max}$  gain compression mechanisms. Average rf gate and drain currents can be used distinguish different gain compression mechanisms such as knee voltage, pinch-off voltage, breakdown voltage and  $I_{max}$  in PHEMT devices.

#### 五.計畫成果與自評

#### 六.參考文獻

[1] C. C. Meng, J. W. Chen, C. H. Chang, L. P. Chen, H. Y. Lee and J. F. Kuan, "Using average RF gate and drain currents to determine gain compression mechanisms for narrow-recessed and wide-recessed MESFETs," *European Gallium Arsenide and other semiconductors application symposium (GAAS 2000)*, p338-341, Oct 2000.

[2] C. C. Meng, C. H. Chang, J. F. Kuan and G. W. Huang, "Direct Observation of Loadlines in MESFET by Using Average RF Gate and Drain Currents", *2002 IEEE international microwave symposium MTT-S*, pp.2161-2164

[3] S.C. Cripps, *RF power amplifiers for wireless communications*, Boston, London: Artech House, 1999.

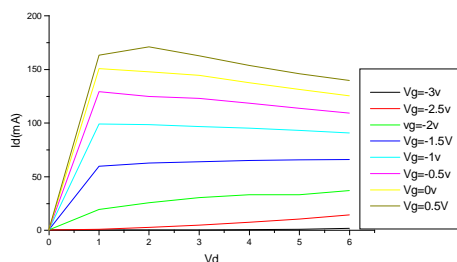


Fig. 1 I-V curves for a high  $V_p$  PHEMT device. Pinch-off voltage is 2.5 V.

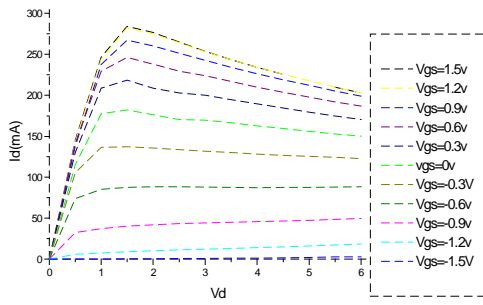


Fig. 2 I-V curves for a low  $V_p$  PHEMT device. Pinch-off voltage is 1.5 V.

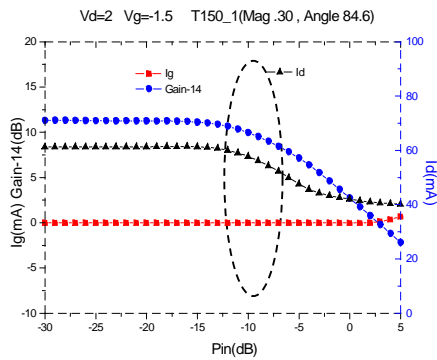


Fig. 3 Gain,  $I_g$  and  $I_d$  vs.  $P_{in}$  for a high  $V_p$  PHEMT device when biased near knee voltage.  $I_g=0$  and  $I_d$  decreases near  $P_{1dB}$ . The gate current is still zero at even higher gain compression point.

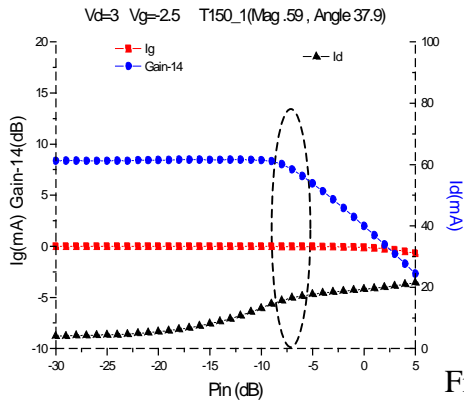


Fig.4 Gain,  $I_g$  and  $I_d$  vs.  $P_{in}$  for a high  $V_p$  PHEMT device when biased near pinch-off voltage.  $I_g=0$  and  $I_d$  increases near  $P_{1dB}$ .

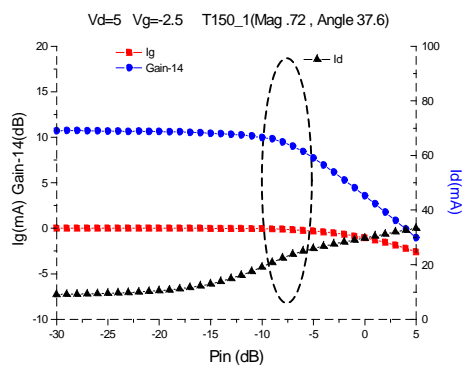


Fig. 5 Gain,  $I_g$  and  $I_d$  vs.  $P_{in}$  for a high  $V_p$  PHEMT device when biased near breakdown voltage.  $I_g < 0$  and  $I_d$  increases near  $P_{1dB}$ .

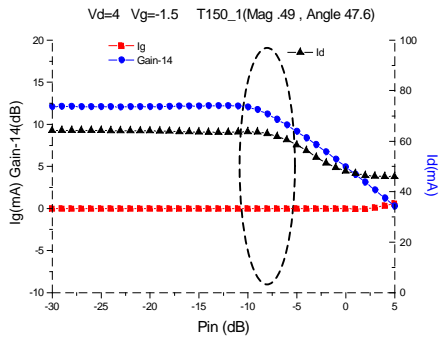


Fig. 6 Gain,  $I_g$  and  $I_d$  vs.  $P_{in}$  for a high  $V_p$  PHEMT device when biased near  $I_{max}$ .  $I_g=0$  and  $I_d$  decreases near  $P_{1dB}$

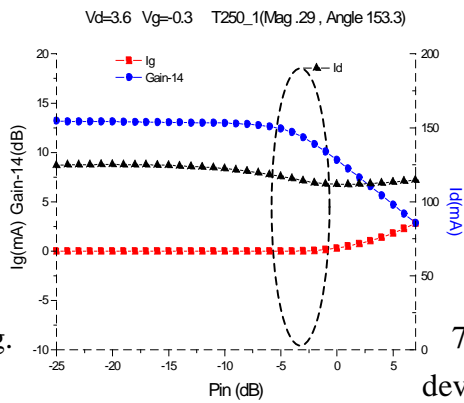


Fig. 7 Gain,  $I_g$  and  $I_d$  vs.  $P_{in}$  for a low  $V_p$  PHEMT device when biased near  $I_{max}$ .  $I_d$  decreases and  $I_g$  increases near  $P_{1dB}$ .

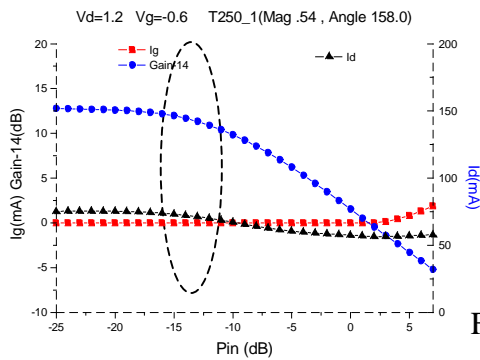


Fig. 8 Gain,  $I_g$  and  $I_d$  vs.  $P_{in}$  for a low  $V_p$  PHEMT device when biased near knee voltage.  $I_d$  decreases and  $I_g=0$  near  $P_{1dB}$ .